REPORT DOCUMENTATION PAGE

AFRL-SR-AR-TR-02-

0098

1. REPORT DATE *(DD-MM-YYYY)*	2. REPORT TYPE	3. DATES COVERED *(From - To)*
09/09/2001	Final	5/1998 - 1/2001

4. TITLE AND SUBTITLE

All Optical Transistors for Ultrafast Computing

5a. CONTRACT NUMBER F49620-98-1-0254

5b. GRANT NUMBER

5c. PROGRAM ELEMENT NUMBER

6. AUTHOR(S)

P. P. Ho and R. R. Alfano

5d. PROJECT NUMBER

5e. TASK NUMBER

5f. WORK UNIT NUMBER

7. PERFORMING ORGANIZATION NAME(S) AND ADDRESS(ES)

The City College of The City University of New York
138th street & Convent Ave
New York, NY 10031

8. PERFORMING ORGANIZATION REPORT NUMBER

9. SPONSORING / MONITORING AGENCY NAME(S) AND ADDRESS(ES)

AFOSR
801 N. Randolph Street Rm732
Arlington, VA 22203-1977

10. SPONSOR/MONITOR'S ACRONYM(S) AFOSR

11. SPONSOR/MONITOR'S REPORT NUMBER(S)

12. DISTRIBUTION / AVAILABILITY STATEMENT

13. SUPPLEMENTARY NOTES

14. ABSTRACT

Information technology is aiming at higher speed, smaller dimensions, and better performance. Basic processes to produce all-optical transistors (OT) based on the novel polarization-controlled all-optical amplifier in non-birefringent single-mode optical fibers to modulate and amplify weak optical signals have been investigated. A weak signal passing into an OT will be amplified using an intense pump optical wave co-propagating in optical fibers. Using a non-birefringent single-mode optical fiber is better because the desired working optical power is much lower than that using a birefringent one because the natural birefringence in a birefringent fiber has to be canceled first by an intense optical wave. We have designed, assembled, and tested a single stage optical transistor based on the polarization controlled optical amplifier approach. Alternative nonlinear optical glasses and liquids with larger x^3 values than the reference CS_2 gate at fast switching speed have been measured by four wave mixing, optical Kerr gate, and z-scan supported by other research grants. The optical nonlinearity and response time of several newly developed optical materials, such as a heavy element doped glass (PbO-Bi2O3-Ga2O3), Tb+3 doped fiber, a silica micro-structured fiber, and Cu doped ZnSe crystals have been studied.

15. SUBJECT TERMS

16. SECURITY CLASSIFICATION OF:			17. LIMITATION OF ABSTRACT	18. NUMBER OF PAGES	19a. NAME OF RESPONSIBLE PERSON
a. REPORT	b. ABSTRACT	c. THIS PAGE			19b. TELEPHONE NUMBER *(include area code)*

INSTRUCTIONS FOR COMPLETING SF 298

1. REPORT DATE. Full publication date, including day, month, if available. Must cite at least the year and be Year 2000 compliant, e.g. 30-06-1998; xx-06-1998-, xx-xx-1998.

2. REPORT TYPE. State the type of report, such as final, technical, interim, memorandum, master's thesis, progress, quarterly, research, special, group study, etc.

3. DATES COVERED. Indicate the time during which the work was performed and the report was written, e.g., Jun 1997 - Jun 1998; 1-10 Jun 1996; May - Nov 1998; Nov 1998.

4. TITLE. Enter title and subtitle with volume number and part number, if applicable. On classified documents, enter the title classification in parentheses.

Ba. CONTRACT NUMBER. Enter all contract numbers as they appear in the report, e.g. F33615-86-C-5169.

5b. GRANT NUMBER. Enter all grant numbers as they appear in the report, e.g. AFOSR-82-1234.

5c. PROGRAM ELEMENT NUMBER. Enter all program element numbers as they appear in the report, e.g. 61101A.

5d. PROJECT NUMBER. Enter all project numbers as they appear in the report, e.g. 1F665702D1257; ILIR.

5e. TASK NUMBER. Enter all task numbers as they appear in the report, e.g. 05; RF0330201; T4112.

5f. WORK UNIT NUMBER. Enter all work unit numbers as they appear in the report, e.g. 001; AFAPL30480105.

6. AUTHOR(S). Enter name(s) of person(s) responsible for writing the report, performing the research, or credited with the content of the report. The form of entry is the last name, first name, middle initial, and additional qualifiers separated by commas, e.g. Smith, Richard, J, Jr.

7. PERFORMING ORGANIZATION NAME(S) AND ADDRESS(ES). Self-explanatory.

8. PERFORMING ORGANIZATION REPORT NUMBER. Enter all unique alphanumeric report numbers assigned by the performing organization, e.g. BRL-1234; AFWL-TR-85-4017-Vol-21-PT-2.

9. SPONSORING/MONITORING AGENCY NAME(S) AND ADDRESS(ES). Enter the name and address of the organization(s) financially responsible for and monitoring the work.

10. SPONSOR/MONITOR'S ACRONYM(S). Enter, if available, e.g. BRL, ARDEC, NADC.

11. SPONSOR/MONITOR'S REPORT NUMBER(S). Enter report number as assigned by the sponsoring/ monitoring agency, if available, e.g. BRL-TR-829; -21 5.

12. DISTRIBUTION/AVAILABILITY STATEMENT. Use agency-mandated availability statements to indicate the public availability or distribution limitations of the report. If additional limitations/ restrictions or special markings are indicated, follow agency authorization procedures, e.g. RD/FRD, PROPIN, ITAR, etc. Include copyright information.

13. SUPPLEMENTARY NOTES. Enter information not included elsewhere such as: prepared in cooperation with; translation of; report supersedes; old edition number, etc.

14. ABSTRACT. A brief (approximately 200 words) factual summary of the most significant information.

15. SUBJECT TERMS. Key words or phrases identifying major concepts in the report.

16. SECURITY CLASSIFICATION. Enter security classification in accordance with security classification regulations, e.g. U, C, S, etc. If this form contains classified information, stamp classification level on the top and bottom of this page.

17. LIMITATION OF ABSTRACT. This block must be completed to assign a distribution limitation to the abstract. Enter UU (Unclassified Unlimited) or SAR (Same as Report). An entry in this block is necessary if the abstract is to be limited.

Research Grant NO. F49620-98-1-0254

BMDO Pilot Program for Science and Technology Research at HBCU/MI

All Optical Transistors for Ultrafast Computing

CBC: Carol Williams, Ballistic Missile Defense Organization Small/Disadvantaged Business Utilization Office, BMDO/TRI, 7100 Defense Pentagon, Washington, D.C.

Final Report (Period: 6/1/98 - 1/31/01)

Submitted to

US Air Force Office of Scientific Research

Prepared by

P. P. Ho and R. R. Alfano

Departments of Electrical Engineering and Physics
The City College of The City University of New York
New York, NY 10031

212-650-6808, 5530 (Fax) e-mail: ho@ccny.cuny.edu

CUNY RF#47395-00-01

2. Objectives

To study the underlying physics, and build and test five different types of all-optical transistors (OT) based on the operation principle of the polarization controlled optical amplification (PCOA). PCOA is based on the cross-phase-modulation (XPM) arising from the third order nonlinear optical process.

We have demonstrated the followings accomplishments in the program objectives:

- Demonstrate past PCOA experiments
- Design OT for the amplification and an logic "AND" gate
- Identifying suitable nonlinear optical materials with larger x^3 to reduce pump power requirements
- Determine signal to noise ratio
- Use ps diode lasers for pump and signal sources
- Recruit and train students in laboratory work and thesis research
- Interact with researchers from DoD and private sectors to obtain design requirements for future OT instrumentation
- Interact with several companies.

3. Summary of Research Program

During the first year, we have designed, assembled, and tested a single stage optical transistor based on the polarization controlled optical amplifier approach. We have identified alternative nonlinear optical glasses and liquids with larger x^3 values than the reference CS_2 gate at fast switching speed measured by four wave mixing, optical Kerr gate, and z-scan supported by other research grants.

During the grant, we have measured the optical nonlinearity and response time of several newly developed optical materials, such as a heavy element doped glass (PbO-Bi2O3-Ga2O3) fabricated by **Corning**, a Tb+3 doped fiber with the length ~ 20 meter obtained from Corning Inc., a silica micro-structured fiber has been obtained from **Lucent Laboratories**, and Cu doped ZnSe crystals were acquired from **Optical Semiconductors, Inc**. The following is a list of x3 nonlinear materials tested for the possible optical transistor operation.

Material	$\Pi^{(3)}$	Switching Time	Figure of Merit ($\Pi^{(3)}/\tau$)
CS_2 [reference]	10^{-12} esu	$2x10^{-12}$ s	~ 1
Silica Glass/Fibers	10^{-14} esu	$< 10^{-14}$ s	> 1
Microstructure Fiber	10^{-14} esu	$< 10^{-14}$ s	> 1
Tb+3 Glass Fiber	10^{-13} esu	TPA*	~ 1
Bismuth Glass	10^{-11} esu	$< 10^{-14}$ s	> 1000
Salol (orientation)	10^{-11} esu	$< 10^{-9}$ s	> 100
ZnSe (Cu+ crystal)	10^{-12} esu	10^{-9} -10^{-14} s	~ 1
ZnSe (amorphous)	10^{-12} esu	10^{-9} -10^{-14} s	~ 1

Two laser systems were used in this project:

Lasers	Pulse Duration	Pulse Energy	Repetition Rate
M-L YAG	30-ps	10-mJ	10-Hz
Ti-sapphire	100-fs	3-uJ	250-KHz
	100-fs	10-nJ	82-MHz

4. Accomplishments/~~New~~ Findings

- **Corning LBG Glass**: Glass is the basic building material for optical communication and other photonic devices. Several research groups have demonstrated that the nonlinear refractive indices of oxide glasses can be increased by addition of heavy-metal-cations, such as Pb, Bi, and Ti. The nonlinear refractive indices of these glasses were measured using the Z-scan, the four-wave mixing, and the third-harmonic generation. In this program, the wavelength dependence of the optical Kerr effect in Lead-Bismuth-Gallate glass was investigated by using 200 fs laser gating pulses. The optical Kerr gating time of 350 fs was obtained at the probe wavelength of 720 nm and the peak Kerr transmitted signal was found to be two times larger than that of the current standard CS_2 Kerr liquid medium. This investigation confirmed that the nonlinear response in LBG glass is mainly derived from electronic origin and this glass material could be adapted for applications in femtosecond optical gate and all optical transistor. (A manuscript submitted to Optical Communications for publication is attached as Appendix 1).

- **Corning Nonlinear Fiber Sample**: A special nonlinear optical fiber obtained from Corning was used to investigate nonlinear optical processes. The negative nonlinear index refraction arising from the heavy element doped fiber may provide a dispersionless property for laser pulses propagating in a long waveguide. This collaboration provided us with various heavy element doped fibers and strengthened the task to identify new PCOA materials with larger and faster nonlinear optical properties than that of silica glasses. Two photon absorption of 1064-nm laser pulse propagating through a Corning supplied Tb doped glass fiber with a high refractive index of 1.78 was measured. The measured output 1064-nm intensity was displayed as a function of the input intensity and the fiber length. In Fig.1 and Fig.2, respectively. The theoretical fitting is consistent with the experimental curve.

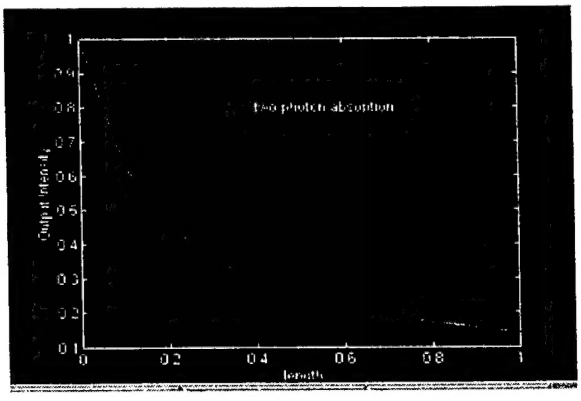

Fig.1 Transmitted 1064-nm signal through a Tb-doped glass fiber as a function of the input intensity.

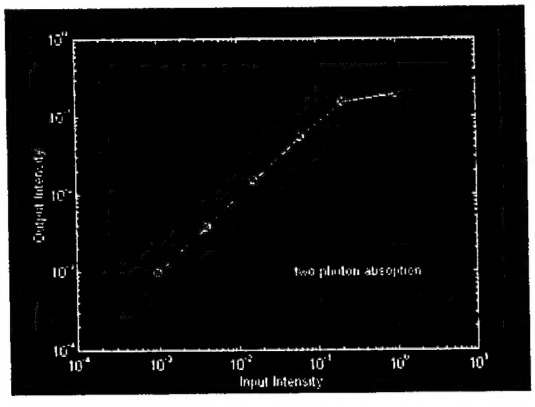

Fig.2 Transmitted 1064-nm signal through a Tb-doped glass fiber as a function of fiber length

It was found that the output spectral distribution generated from SPM in this Tb doped Corning fiber is non-symmetric in comparison with a conventional Newport optical fiber. This behavior can be theoretically fitted with a non-symmetrical Gaussian temporal pulse profile propagating through this fiber.

- **Lucent's Micro-structured Fiber** (Holy Fiber)

The intensity dependence of the supercontinuum generation in silica glass based micro-structure fiber supplied by Lucent Technology's Dr. R. Windeler has been investigated as a function of fiber length. The experimental arrangement is displayed in the left figure. On account of the negative chirped waveguide dispersion in compensation with the positive chirped material dispersion in the air-silica microstructure, the effective refractive index is nearly the same over the entire wavelength span from 500-nm to 1500-nm. The conversion efficiency and the intensity uniformity of the continuum generation output by passing through a femtosecond laser pulse through a one meter long microstructure fiber have been significantly improved. Nonlinear optical effects of pulse propagation through the microstructure fiber from the violet to the infrared have been investigated from the self-phase-modulation (SPM), second harmonic generation (SHG), SHG-SPM, four-wave-mixing (FWM), and cross-phase-modulation (XPM) processes.

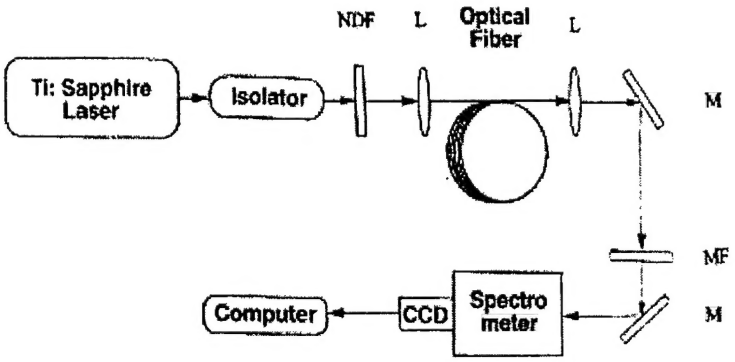

Experimental Setup

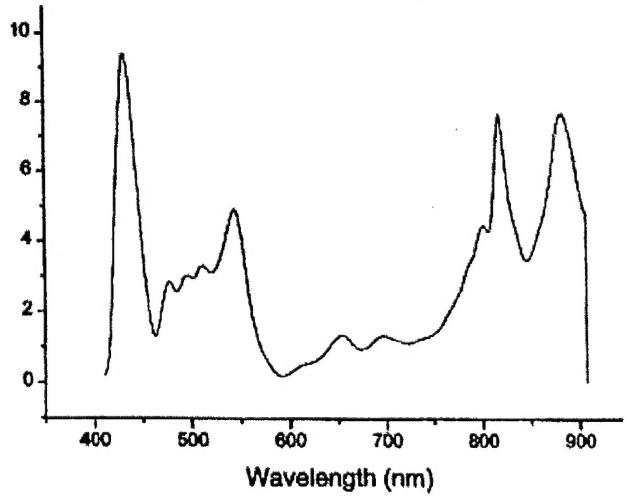

A measured supercontinuum output spectrum from an incident 60-picos-Joules 100-fs at 800-nm is displayed in below. Most input pulse energy at 800-nm has been converted into a broader band output laser. The sharp peak at 400-nm is the SHG, the second broadband output from 460-nm to 570-nm can be accounted for the SHG-XPM, and the peak at 880-nm is attributed to FWM. Spectrum above 900-nm was cutoff from the measurement sensitivity.

- **ZnSe Nonlinear Pulse Shaping**: Optical Semiconductors, Inc. measured and modeled two photon absorption and dispersion in x3 nonlinear materials. The mechanism of the polarization controlled optical amplification has been clarified, which depends on the nonlinear dispersion in the third order nonlinear optical process but not the cross-phase-modulation. Using the following equation, the cross-phase-modulation arising from the third

order nonlinearity and the amplification/absorption arising from the third nonlinear dispersion can be described.

$$\frac{\partial}{\partial z}(E_s+E_p)\cong i\frac{2\pi\varepsilon_0}{kc^2}\omega^2\chi^{(3)}\left|E_s+E_p\right|^2(E_s+E_p)+\frac{2\pi\varepsilon_0}{kc^2}\frac{\partial[\omega^2\chi^{(3)}]}{\partial\omega}\frac{\partial}{\partial t}\left(\left|E_s+E_p\right|^2(E_s+E_p)\right),$$

where the first term and the second term in the right hand represent the phase modulation and the energy transfer. For the polarization controlled optical amplification,

$$\frac{\partial}{\partial z}E_s\propto\frac{2\pi\varepsilon_0}{kc^2}\frac{\partial[\omega^2\chi^{(3)}]}{\partial\omega}E_s\frac{\partial}{\partial t}\left|E_p\right|^2 \quad .$$

In some semiconductor materials, such as ZnSe, there is a large nonlinear dispersion. It can be used to amplify the infrared signal (1064nm) while the green light (532nm) pumping exists. In addition, there is also a large optical nonlinear dispersion in some doped optical fibers.

A manuscript was accepted by Optics Communications for publication (See Appendix 2).

5. Personnel Supported Two faculty PIs: Prof. Ho and Prof. Alfano were supported by this grant at 10% effort during the academic year and 0.5 months during the summer. One full-time researcher (G. Tang) and one part-time student (Cindy Navah) were supported by this grant to conduct the proposed tasks. The following personnel listed below were supported by other research grants from NASA, NYS/CAT, AF Wright Lab. to assist in several relevant tasks:

Researcher	Supported by	Tasks
G. Bai	AF Wright Lab.	Induced Beam Deflectors
A. Bykov	NYS/CAT	Material Growth
J. Ying	NASA	Nonlinear Optical Fibers
K. Sutkus	NASA	ps Diode Lasers

6. Publications

- Submitted a paper to Optics Communications entitled "Femtosecond optical Kerr gate using Pb0-Bi_2O_3-Ga_2O_3 doped glasses" by B. Yu, T. Qiu, A. Bykov, P. Ho, and R. Alfano.
- Submitted a paper to Optics Communications entitled "Intensity-dependent temporal laser pulse shaping and propagation in ZnSe" by Y. Bai, P. Ho, and R. Alfano.
- Presented a paper at 1998 OSA annual meeting (Time-resolved FWM on nonlinear optical materials), Oct. 1998
- Presented a paper at 1999 CLEO (Femtosecond optical Kerr gate), May 1999.
- Presented a paper at 2000 OSA annual meeting (Nonlinear optical processes in micro-structured fibers), Oct. 2000.

7. Interaction

- Collaborated with Dr. Borelli's group at Corning Inc. to investigate nonlinear optical processed in heavy element doped fibers.

- Collaborated with Dr. Fitzpatrick of Optical Semiconductors, Inc. to investigate nonlinear optical process of Cu doped ZnSe crystals.

- Collaborated with Dr. Windeler of Lucent Technology to investigate nonlinear optical process of silica micro-structured fibers (Holy fibers).

8. New discoveries or Patent Disclosure

none

Appendix 1: Research Grant NO. F49620-98-1-0254

Femtosecond Optical Kerr Shutter Using Lead-Bismuth-Gallium Oxide Glass

B.Yu, T. Qiu, A. B. Bykov, P. P. Ho, R. R. Alfano

Departments of Physics and Electrical Engineering, New York State Center for Advanced Technology for Ultrafast Photonic Materials and Applications, The City College of The City University of New York, New York, NY 10031

N. Borrelli

Corning Incorporated SP-FR-3-1, Corning NY 14831

Abstract

A femtosecond Kerr shutter was demonstrated in a lead-bismuth-gallate glass. The optical gating time was measured to be less than 350 fs and the peak Kerr transmitted signal was found to be 2.3 larger than that of the current standard CS_2 liquid medium.

Key words: Optical Kerr gate, Ultrafast shutter, Nonlinear optical material

OCIS codes: 190.3270; 190.7110; 190.4400

320.0320; 320.2250; 320.711

Corresponding author: Prof. R. R. Alfano

Email: alfano@scisun.sci.ccny.cuny.edu. Tel : 212-650-5531, Fax: 212-650-5530

*IUSL#02-01 Submitted to Optics Communications, Jan. 2002

1. Introduction

Photonic devices consist of nonlinear optical gates and logic circuits based on the third order susceptibility ($\chi^{(3)}$) promises the ultimate switching speed for uses in the computation and the communication fields. The optical Kerr gate(OKG)[1-5] has been used as an ultrafast gate for time-resolved biomedical optical imaging and optical interconnect applications. One key advantage of the OKG is the capability to acquire a time sliced true 2D spatial image for both incoherent and coherent optical signals. Carbon disulfide (CS_2) liquid with the $\chi^{(3)}$ value ~10^{-13} esu in femtosecond time scale is commonly used as the standard OKG switching medium. Several other future applications in ultrafast photonic devices like the induced optical beam deflector [6], optical analog to digital converters [7], and optical transistor amplifiers require $\chi^{(3)}$ materials with fs response time and large Kerr coefficient [8]. Over the past twenty years, the bottleneck for implementing $\chi^{(3)}$ based ultrafast photonic devices is the size of $\chi^{(3)}$ value to reduce the input power requirement to generate the desired nonlinear optical process. New materials [8-14] with a large optical nonlinearity and a fast response time are crucial for the implementation of these new technologies.

For most commonly known nonlinear optical materials in the visible and NIL regimes, their non-resonant $\chi^{(3)}$ values are in the range of ~10^{-14} esu (silica glass, fs response time) to ~ 10^{-12} esu. Several semiconductors, organic or polymeric materials seem to have very large $\chi^{(3)}$ values [10, 11, 15], however, these materials are limited by either being too thin, consisting of diluted nonlinear active molecules in a host medium, or having a slow response time. After taking these factors in account, such as the sample thickness (z), concentration (n), and response time (τ), the effective induced nonlinear

refractive index change ($\chi^{(3)}$ nz / τ) from the CS_2 liquid is still the best nonlinear optical material in the ps time regime. For many ultrafast applications, a new nonlinear material with a larger Kerr constant with fs response time is needed.

Among the potential nonlinear optical materials, glasses have the advantages of easy fabrication, high transparency, high chemical and thermal durability, and high optical damage resistance. Glass is the basic block building material for optical communication and other photonic devices. Several research groups [12-14] have demonstrated that the nonlinear refractive indices of oxide glasses can be increased by addition of heavy-metal-cations, such as Pb, Bi, and Ti. The nonlinear refractive indices of these glasses were measured using the Z-scan [12], the four-wave mixing [13], and the third-harmonic generation [14]. The $\chi^{(3)}$ values measured at wavelength of 600 nm for $Ti_2O(30)Bi_2O_3(20)$ glass and $La_2S_3(35)Ga_2S_3(65)$ glass were ~5.2 and 2.9×10^{-11} esu, respectively. These $\chi^{(3)}$ values are more than ten times larger than the $\chi^{(3)}$ from the CS_2 and are more than 1,000 times larger than the $\chi^{(3)}$ from a convention glass or silica fibers. Ultrafast photon switching devices using optical fibers and waveguide structures made of these heavy element doped glasses should use much less power than conventional silica fibers.

In this article, the response time and dispersion of the optical Kerr gate from a heavy element doped lead-bismuth-gallium $PbO\text{-}Bi_2O_3\text{-}Ga_2O_3$ (LBG) glass were determined using a high repetition rate Ti: sapphire fs laser pulse. The $\chi^{(3)}$ value of this glass gated at 800 nm and probed with a supercontinnum source in the non-resonant region was ~ 10^{-13} esu with ~ 200 fs response. The OKG measurement and supercontinuum source were conducted to bring out time response and dispersion of

OKG in LBG glass. The Kerr response time was obtained using different wavelengths generated from a supercontinuum to avoid the coherent artificial effect [3].

2. Experimental

Heavy-metal oxide LBG glasses were fabricated by melting mixtures of Pb_3O_4, Bi_2O_3 and Ga_2O_3 at 900 °C in a gold crucible in air from either in house or supplied by Corning Inc. The melt was then cast onto a bronze plate and annealed at 350 °C for several hours. The composition of the LBG glass was ~ 40%PbO-35%$BiO_{1.5}$-25%$GaO_{1.5}$. The sample was cut to a 1mm thick plate and polished in both surfaces for optical measurements. The absorption spectrum of the glass was measured and exhibited good transparency in the spectrum range more than 600 nm and the absorption edge was at ~500 nm (Fig. 1).

The experimental setup of the fs Optical Kerr gate is shown in Fig.2. A laser pulse train with 200 fs pulse duration at 800 nm operating at 250 kHz was obtained from a regenerated amplified Ti: sapphire laser system. The pulse average energy was ~ 3μJ. The input beam of the laser was split into two parts, one beam was used as the gating beam, the other as the probe beam. The gating pulses induce transient birefringence in the nonlinear glass and cause the polarization change of the probe light. To prevent the effects of the "coherent artifact" [10] in OKG, the wavelength of the probe beam was chosen to be different from the gating beam. This is achieved by focusing the probe beam into a piece of 1cm thickness BK7 glass plate to generate supercontinuum [16-18]. The desired wavelength of the probe beam was extracted from the supercontinuum using a narrow band filter with a 10 nm spectral transmission width. In most of our

experiment, 720 nm was used as the probe wavelength which is far enough from the gating beam to avoid the coherent interference while close enough to minimize the dispersion which can broaden the gating time width. The intensity of the probe pulses is kept to be small in compared to the gating pulses (ratio ~ $1:10^4$). To avoid the saturation effect [9] and the nonlinear absorption [20] in the OKG, the gating intensity at the Kerr cell was set to be less than 3 GW / cm^2. The Kerr sample was positioned between a polarizer and an analyzer in a cross Nicoal configuration. The time delay between gating and probe pulses was controlled by a stepping-motor with a minimum temporal resolution to be ~ 6.67 fs.

3. Experimental results

The measured time-resolved transmission signals of the OKG using the LBG glass gate is shown in Fig. 3. The gating pulse wavelength was at 800 nm and the probe pulse wavelength was at 720 nm. For the comparison purposes, a standard CS_2 OKG measurement is also displayed in Fig. 3. The liquid CS_2 was situated in a 1.0 mm thick cell. Both samples were measured under the same gating and probe power condition. The salient feature of this figure indicates that the temporal profile of OKG in from the LBG glass is asymmetrical with the FWHM of ~ 350 fs while the CS_2 gate has an asymmetrical decay tall with ~ 1.6 ps decay time attributed to the re-orientational relaxation process [1-5]. The peak transmission efficiency from the glass OKG raw data was ~ 2.3 times larger than that from a CS_2 gate.

In addition, the measured gate opening times of the time-resolved OKG transmission signal for different probe wavelengths from 720 nm to 520 nm are displayed in Fig. 4.

When the probe wavelength was shorter, besides the time delay of the peak transmitted signal due to the normal dispersion of the supercontinuum generation, the gating FWHM time was also found to increase from 350 fs to 2.5 ps. The increasing of the gating width is attributed to the dispersion of the supercontinuum generation medium [22] and the mixing of the four-wave-mixing signal [18, 23].

To compare the absolute value of the Kerr nonlinearity $\chi^{(3)}$ of the LBG glass used in the OKG with a standard CS_2 OKG, an empirical equation was used under the same experimental condition. The following equation was employed to calculate LBG $\chi^{(3)}$.

$$\chi_S^{(3)} = \chi_R^{(3)} \left(\frac{I_S}{I_R} \right)^{1/2} \left(\frac{n_S}{n_R} \right)^2 , (1)$$

The subscripts S and R represent the sample of LBG glass and reference sample CS_2. I indicates the intensity of OKG and n is the refractive index. The $\chi^{(3)}$ for CS_2 is 1×10^{-13} esu in femtosecond time scale [24, 25]. By the measurement of the peak transmitted signal at the zero delayed in Fig.3 and considering the surface refraction loss from the gating sample due to the different linear refractive index [n(glass) ~ 2.3, n(CS_2) ~ 1.62] from both the gating beam(800 nm) and the probe beam(720 nm), $\chi^{(3)}_S / \chi^{(3)}_R \sim 3$ was obtained.

Figure 5 gives the probe transmittance as a function of the gating intensity at 720 nm. The result of carbon disulfide was also shown in the figure for comparison. The probe transmittance (T) of the LBG glass measurement is given by

$$T = T_0 \left(\frac{24\pi^2 L_{eff} \chi^{(3)}}{n_S^2 a C \lambda_p} \right)^2 P_g^2 , (2)$$

where $P_g = I_g / \pi a^2$ (I_g: gate intensity; a: beam radius at the focal point). T_0 is the transmissivity for open-Nicol configuration, L_{eff} is the effective length of the sample, C is the velocity of light and λ_p is the wavelength of probe beam. From Fig. 5, below the gate intensity of 3.0 GW /cm^2, the measured values of the transmittance increase in proportion to the square of I_g as expected from Eq. (2). When the gating intensity is the same, the LBG glass shows about 2.3 times large than that of CS_2. This result is consistent with the OKG in the LBG glass measurements shown in Fig. 3. The nonlinear optical response of LBG glass arises mainly from electron cloud distortion.

4. Summary

The transient OKG signal from the LBG Kerr gate at 720 nm was found to be 350 fs and the absolute transmitted signal at 720 nm was more than 2 times larger than that from a CS_2 gate. The experiments in this investigation confirmed that the nonlinear response in LBG glass is mainly derived from electronic origin and suggests a potential application in femtosecond Kerr shutter for all optical switching..

ACKNOWLEDGMENT This research is supported in part by Air Force Wright Laboratory, AFOSR / BMDO, New York State Science and Technology Foundation, and NASA / IRA Program. We thank Prof. W. LaCourse of Alfred University for supplying the sample.

References

[1] P. Ho and R. R. Alfano, Phys. Rev. A 20(1978)2170-2183.

[2] " Picosecond Kerr gate", P. Ho, in " Semiconductor processes probed by ultrafast laser", ed. by Alfano, Ch. 25, 410-439, Academy Prsss, 1984.

[3] B. I. Greene and R. C. Farrow, Chem. Phys. Lett. 98(1983) 273-272.

[4] C. Kalpouzos, W. T. Lotshaw, D. McMorrow, G. A. Kenney-Wallace, J. Phys. Chem., 91(1987)2028-2030.

[5] Hirohisa Kanbara, Seiji fujiwara, Koichiro Tanaka, Hiroyuki Nasu, and Kazuyuki Hiro, Appl. Phys. Lett., 70(1997)925-927.

[6] P. Ho, Q. Wang, J. Chen, Q. Liu, R. R. Alfano, Appl. Opt., 36(1997)3425-3430.

[7] P. Ho, Q. Wang, and R. R. Alfano, SPIE 2155(1994)157-161.

[8] G. Jonusauskas, J. Oberle, E. Abraham, and C. Rulliere, Opt. Commun., 137(1997) 199-206.

[9] N. Peyghambarian, S. W. Koch, and A. Mysyrowicz, Iintroductor to Semiconductor Optics(Prentice-Hall, Englewood Cliffs, NJ), 1993.

[10] S. R. Friberg and P. W. Smith, IEEE J. Quantum Electronics, QE-23(1987)2089-2093.

[11] D. Williams ed, "Nonlinear optical properties of organic and polymeric materials", Am. Chem. Society, Washington, DC, 1983.

[12] D. Auston, Appl. Opt., 26(1987)211-221.

[13] I. kang, T. D. Krauss, F. W. Wise, B. G. Aitken, and N. F. Borrelli, J. Opt. Soc. Am. B12(1995)2053-2059.

[14] J. Yumto, S. G. Lee, B. Kippelen, N. Peyghambarian, B. G. aitken, and N. F.

Borrelli, Appl. Phys. Lett., 63(1993)2630-2632.

[15] H. Kobayashi, M. Koga, M. Kubodera, J. Appl. Phys., 74(1993)3683-3686.

[16] P. Ho, N. Yang, G. Eichman, and R. R. Alfano, SPIE 682, 36-42(1986).

[17] N. Sugimoto, H. Kanbara, S. Fujiwara, and K. Tanaka, Opt. Lett., 21(1986)1737-1739.

[17] E. P. Ippen and C. V. Shank, in Ultrashort Light Pulses, Ed. S. L. Shapiro(Springer, New York), p. 83, 1977.

[18] R. R. Alfano ed. "The Supercontinuum Laser Source"(Springer-Verlag, New York), Chap. 2, 1989.

[19] R. R. Alfano and P. Ho, IEEE J. of Quantum Electronics, GE-22(1988)351-362.

[20] P. Ho, P. Lu, and R. R. Alfano, Phys. Rev.A, 21(1980)1730-1734.

[21] P. Ho, P. Lu, and R. R. Alfano, J. Chem. Phys., 74(1981)1605-1609.

[22] Q. Li, T. Jimbo, P. Ho, And R. R. Alfano, Appl. Opt., 12(1986)1869-1871.

[23] R. R. Alfano and S. L. Shapiro, Phys. Rev. Lett., 24(1970)592-594.

[24] K. Minoshima, M. Taiji, and T. Kobayashi, Opt. Lett., 16(1991)1683-1685.

[25] Y. Kondo, H. Inouye, S. Fujiwara, T. Suzuki, and T. Mitsuyu, J. Appl. Phys., 88(2000)1244-1227.

Captions

Fig. 1. Absorption spectra of a LBG glass.

Fig. 2. The experimental setup for the time-resolved optical Kerr shutter system. The gating beam is the regenerative amplified Ti: sapphire laser. BK7: a glass with the thickness of 10 mm to generate supercontinuum pulses. $\lambda / 2$: a half wave plate inserted into the probe beam after the supercontinuum generation to minimize the 50 % loss from the 45° first polarizer.

Fig.3 Experimental measurements of LGB glass using time resolved OKG and compared with a CS_2 gate. The horizontal axis is the time delay between the gating and the probe pulse and the vertical axis is the probe pulse intensity at different gating times.

Fig. 4. Measured gate opening time of an OKG using a LBG glass Kerr medium as a function of the probing wavelength. The vertical axis is the measured FWHM of the LBG glass OKG gating time from various transmitted signal using fs supercontinuum. The horizontal axis is the probing wavelength selected by a 10 nm narrow band filter from the supercontinuum generation in BK7 glass excited by 200 fs laser pulses at 800 nm.

Fig. 5. Probe transmittance (T) measured at 720 nm as a function of the gating intensity. When the gating intensity decreases, the probe transmittance increases in proportion to the square gating intensity.

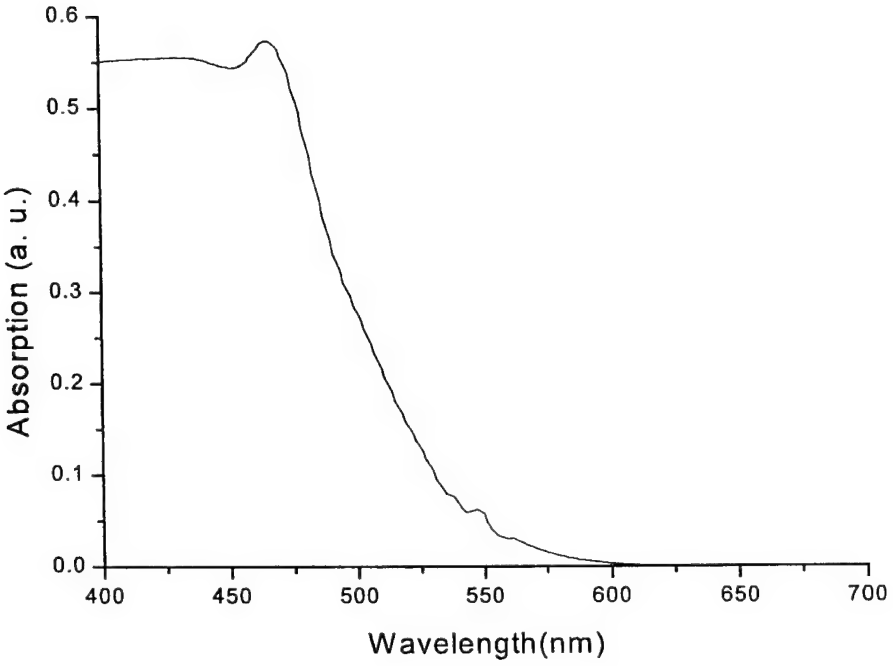
Absorption (a. u.)
0.0
0.1
0.2
0.3
0.4
0.5
0.6
400
450
500
550
600
650
700
Wavelength(nm)

B. Yu

Fig. 1

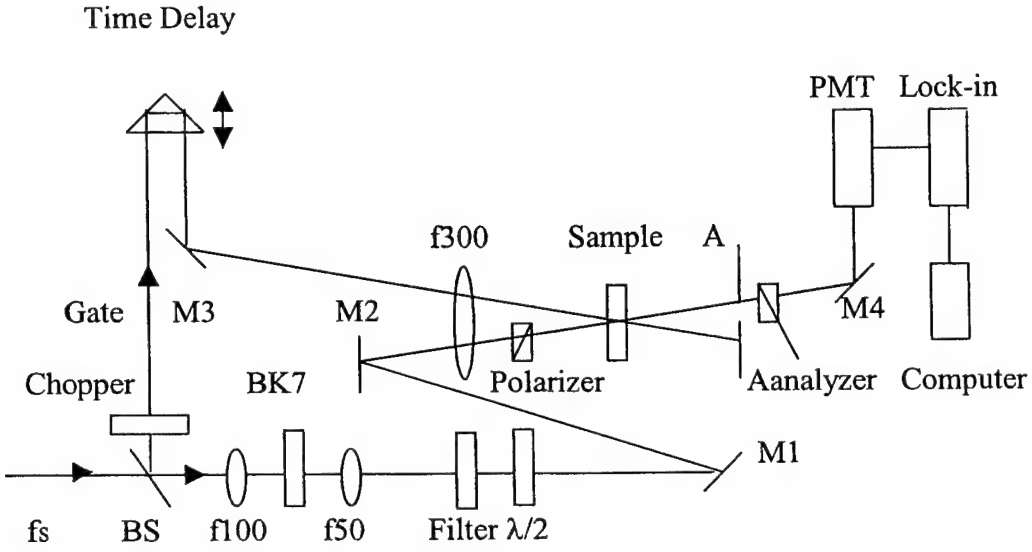
Time Delay
PMT
Lock-in
f300
Sample
A
Gate
M3
M2
M4
Chopper
BK7
Polarizer
Aanalyzer
Computer
M1
fs
BS
f100
f50
Filter λ/2

B. Yu

Fig.2

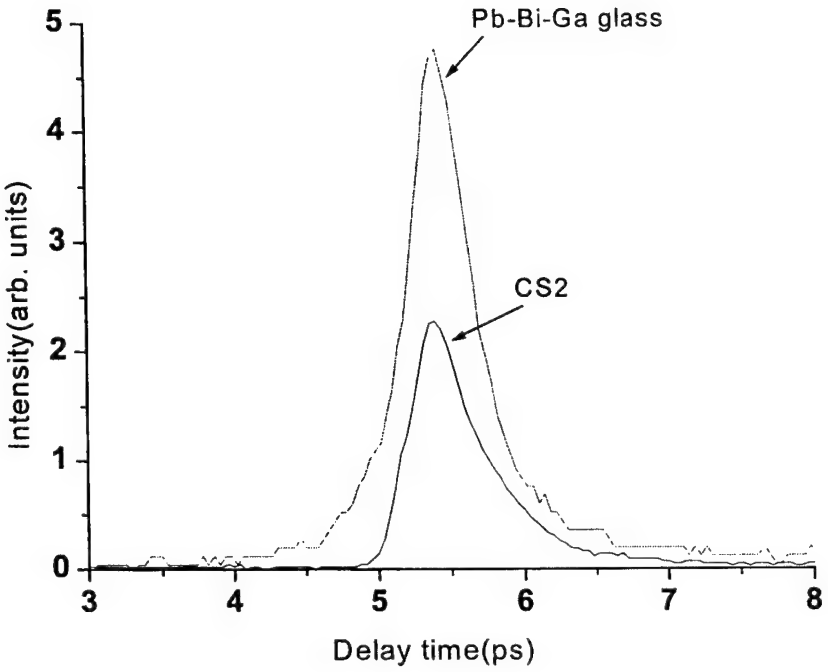
Pb-Bi-Ga glass
CS2
Intensity(arb. units)
Delay time(ps)
0
1
2
3
4
5
3
4
5
6
7
8

B. Yu

Fig. 3

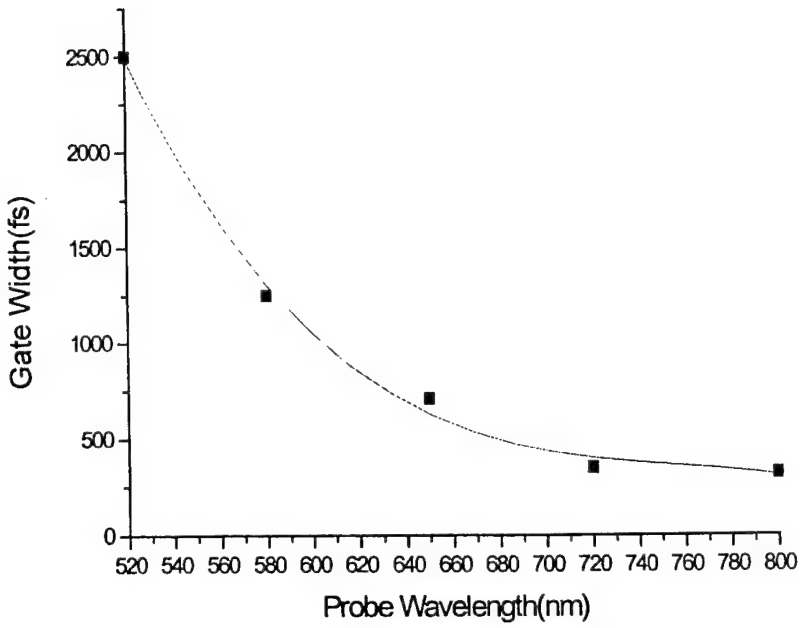
Gate Width(fs)
2500
2000
1500
1000
500
0
520 540 560 580 600 620 640 660 680 700 720 740 760 780 800
Probe Wavelength(nm)

B. Yu

Fig.4

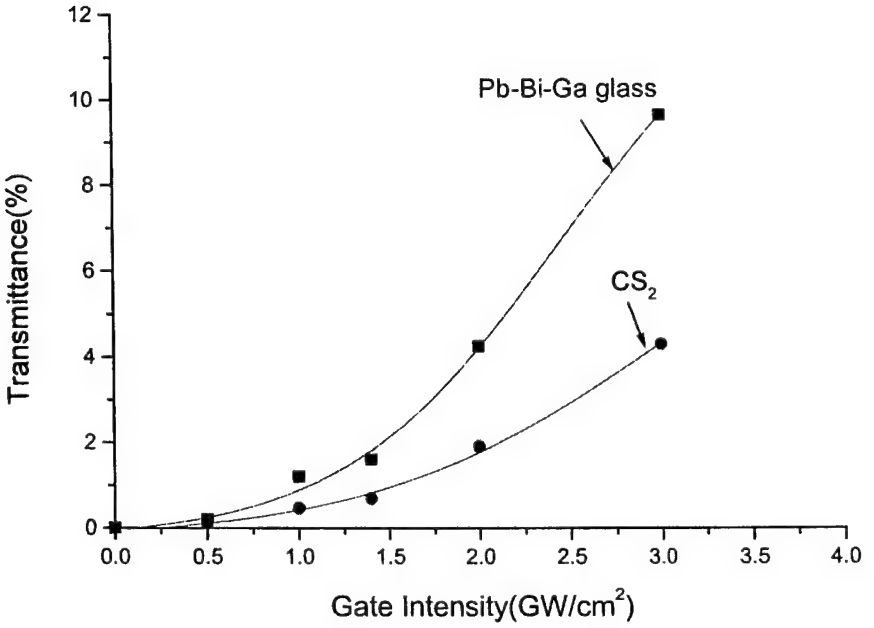
Pb-Bi-Ga glass
CS_2
Transmittance(%)
Gate Intensity(GW/cm^2)
0
2
4
6
8
10
12
0.0
0.5
1.0
1.5
2.0
2.5
3.0
3.5
4.0

B. Yu

Fig. 5

Appendix 2: Research Grant No. F49620-98-1-0254

Intensity-dependent temporal laser pulse shaping and propagation in ZnSe

Yingxin Bai, P. P. Ho, and R.R. Alfano

The Institute for Ultrafast Spectroscopy and Lasers

Departments of Electrical Engineering and Physics

The City College of New York

138th Street and Convent Avenue, New York, NY10031

Abstract

The shape of a 40-ps 1064-nm laser pulse propagating through ZnSe at different intensities was investigated using a single-shot optical Kerr gate. The pulse peak moves forward in time by about 15 ps and the full width at half maximum reduces from 40 ps to 27 ps when the peak intensity of the incident pulse reaches 3.65 GW/cm^2. This pulse advancement and time shortening are attributed to a combination of two-step absorption and negative nonlinear dispersion. The numerically simulated results are in agreement with the experimental ones.

Optics Communication (accepted for publication)

IUSL No: 2000-16

II-VI semiconductors are important materials for many photonic applications. ZnSe has excellent physical, chemical and nonlinear optical properties as well as low absorption spanning from the red to the infrared. Consequently, it is thought of as one of the most promising optical materials for many practical optical functions, such as optical limiting, all-optical switching, displays, tera hertz generation and optical memory elements.[1-6] An anomalous spectral broadening has been observed in ZnSe, larger for Stokes than anti-Stokes.[7] In this paper, the intensity-dependent reshaping of a 40-ps laser pulse through a ZnSe plate was investigated using an improved single-shot optical Kerr gate. Based on our presented model, the two-step absorption with negative nonlinear dispersion, the corresponding numerical simulation was completed.

The schematic arrangement for a single-shot optical Kerr gate (SOKG) technique is shown in Fig.1. A mode-locked Nd:YAG laser was used to generate 1064-nm and 532-nm pulses of 40 ps and 30 ps, respectively. The 30-ps 532-nm probe pulse was passed onto a ~ 90° blazed reflection grating to be transformed into a ~45° oblique temporal front covering a 200-ps temporal window. A lens was used to focus the probe beam into a 1-mm long CS_2 Kerr cell to form an extended probing time base. For a 6-cm length grating, the probing time base covered ~200 ps. Another lens collected the transmitted beam and focused it onto a CCD camera for analysis. The channel/pixel number of the CCD camera displayed the time is 1,024. In this manner, ~ 1,000 times divided data signals can be displayed for a single probing pulse to accurately monitor the temporal profile of the 1064-nm pulse offering a continuous display of the profile. The salient function of the blazed grating was also to compensate the probing pulse chirp due to the

nonlinearity of the amplifier.[8] The probing pulse spectral width measured by a Jarrell-Ash scanning spectrometer was ~6.5 Å. The calculated minimum duration of the oblique front at given time was about 5 ps. The time covered by a CCD channel was 0.2 ps. Including the response time of the CS_2 Kerr medium, ~2 ps, this SOKG approach can measure the shape of a laser pulse (FWHM ~ 40 ps) with about 8-ps temporal resolution over a 200-ps time window.

Using a conventional OKG to measure the temporal profile of one pulse requires the movement a delay device to change the delay path between the gating and the probing pulses, and requires a large number of independent movements to form a profile.[9] Neglecting the response time of the Kerr medium, the minimum temporal resolution is determined by the time convolution of the gating pulse and the probing pulse for a conventional OKG. For the gating pulse of 40 ps and the probing pulse of 30 ps, the minimum time resolution is ~ 1.4 times the FWHM of the gating pulse (the time convolution of the signal pulse and the gate pulse with ~ the same pulse width) which is 42 ps.

The pulse profile measurements for propagation through a ZnSe plate were performed to determine the pulse reshaping arising from nonlinear intensity dependent processes. A set of neutral density filters (F) was used to control the power density for the 1064-nm pulse passing through the ZnSe plate. Neutral density filters were systematically switched between the entrance site and the exit site of the ZnSe sample. In this way, the 1064-nm intensity at ZnSe was varied, while the total linear loss and the time delay of the experimental conditions were maintained to be about the same.

The measured SOKG temporal profiles of the transmitted 1064-nm pulse for incident pulses of three different peak-power-densities: 0.365 GW/cm^2, 1.46 GW/cm^2 and 3.65 GW/cm^2, are displayed in Fig.2. Intensity-dependent pulse shaping was observed. The salient features shown in Fig.2 are pulse advancement and temporal pulse width shortening at high intensity. From 0.365 GW/cm^2 to1.46 GW/cm^2, there was no profile distortion. From 1.46 GW/cm^2 to 3.65 GW/cm^2, the trailing portion of the original profile almost completely disappeared. In addition, (at 3.65 GW/cm^2) the profile peak moved forward ~15 ps and the FWHM was reduced to ~27 ps.

A 3-mm glass plate was used as a reference transparent optical material with a small $\chi^{(3)}$ nonlinearity,. The measured temporal profiles for incident pulses with similar peak-power-densities are shown in the upper left insert of Fig.2. These profiles seem to coincide without any pulse peak-shift and pulse compression. It shows good alignment of the experimental setup and good stability of the laser system. Using a 1-mm CS_2 cell instead of the ZnSe sample, changes in the measured profile were observed without pulse shaping. These changes originated from the self-focusing caused by the nonlinearity in CS_2. The observations in ZnSe imply that the pulse shaping does not only depend on the Kerr nonlinearity.

Typically, the nonlinear absorption of the 1064-nm laser by a pure ZnSe sample occurs by three-photon absorption because of its large band-gap energy of ~ 2.68 eV (λ=460 nm). However, for the ZnSe sample used in this experiment, a commercial amorphous window, the transmission spectrum of this 3-mm thick ZnSe sample measured by a Perkin-Elmer Lambda 9 spectrometer is shown in the upper right insert of

Fig.2. Due to the large interface reflections of ZnSe, the measured transmissivities at 532 nm and 1064 nm are 52.85% and 67.31%, respectively. Taking into account the influence of surface reflection of ZnSe, the transmission at 532 nm is ~10%, while the absorption at 1064 nm is almost 0%. Since a strong absorption exists at 532 nm near the turning point of the transmission curve, two-photon absorption of 1064 nm in this ZnSe window sample is expected from tailing states.

For an incident pulse with the peak-power-intensity of 3.65GW/cm^2, the instantaneous transmitted intensity of a single pulse with this incident intensity is shown in Fig.3. This curve shows the difference in the output profile with intensity at different times with the pulse window. The transmission is the two-valued function of intensity. It indicates an operative complex nonlinear process. The transmission of the early leading part of the incident pulse is linear at the intensity level lower than 1.5GW/cm^2. As the time of the intensity increases to the peak value, the transmitted intensity decreases and the trailing part of the pulse almost disappeared. Therefore, the nonlinear absorption of the1064-nm laser pulse through ZnSe is not a simple two-/three-photon absorption because the nonlinear absorption not only depends on intensity but also depends on time. The observed pulse shortening cannot be interpreted by a simple two-/three-photon absorption because two-/three-photon absorption at the center of pulse is larger than at the wings causing a time broadening.

The intensity-dependent peak-shift of the laser pulse through ZnSe is attributed to intensity-dependent group-velocity. Using the expression for the intensity-dependent group-velocity,[10] the measured peak-shift of $\Delta\tau = -15$ ps, and the known Kerr

nonlinearity,[4] $n_2(1064nm)=170\times10^{-9}$esu, the nonlinear dispersion can be calculated to be $\partial n_2/\partial\omega\approx -1.53\times10^{-29}\,m^2s/W$.

To explain the two salient features observed at high pulse energy, pulse advancement and pulse shortening, we present a model of two-step absorption with negative nonlinear dispersion. The energy level diagram of two-step absorption is illustrated in the insert of Fig.4. Negative nonlinear dispersion results in the advancement and the leading edge steepening of the propagating pulse because the intensity-dependent group-velocity depends on nonlinearity and nonlinear dispersion.[10] The two-step process includes the single-photon absorption from a metastable state (one of gap states) populated by two-photon excitation. In this manner, two-step absorption results in the reduction of trailing portion of the propagating pulse because the linear absorption relies on the population in the metastable state excited by two-photon absorption from the leading edge photons.[11] The leading edge steepening and the reduction of the trailing portion of propagating pulse combine to produce the pulse shortening.

The two-step absorption with negative nonlinear dispersion can be described by following rate equations,

$$\frac{\partial}{\partial\tau}N_0=-\frac{1}{2}\sigma_{01}^{(2)}(N_0-N_1)I^2+\frac{1}{T_{10}}N_1+\frac{1}{T_{20}}N_2, \tag{1}$$

$$\frac{\partial}{\partial\tau}N_1=\frac{1}{2}\sigma_{01}^{(2)}(N_0-N_1)I^2-\frac{1}{T_{10}}N_1-\sigma_{12}^{(1)}(N_1-N_2)I+\frac{1}{T_{21}}N_2, \tag{2}$$

$$\frac{\partial}{\partial\tau}N_2=\sigma_{12}^{(1)}(N_1-N_2)I-\frac{1}{T_{21}}N_2-\frac{1}{T_{20}}N_2, \tag{3}$$

$$\frac{\partial}{\partial \xi} I = -\sigma_{01}^{(2)}(N_0 - N_1)I^2 - \sigma_{12}^{(1)}(N_1 - N_2)I - \delta_{01}^{(2)}(N_0 - N_1)I\frac{\partial}{\partial \tau} I - \delta_{12}^{(1)}(N_1 - N_2)\frac{\partial}{\partial \tau} I,$$

(4)

where the total occupation-number density is constant, $N = N_0 + N_1 + N_2$, and N_0, N_1 and N_2 are the occupation-number densities of the valence band, the gap states and the conduction band, respectively, I is the intensity of laser pulse, $\sigma_{01}^{(2)}$ is the cross section of two-photon absorption, $\sigma_{12}^{(1)}$ is the cross section of gap states absorption, $\delta_{01}^{(2)}$ is the additional nonlinear dispersion coefficient due to two-photon absorption, $\delta_{12}^{(1)}$ is the additional linear dispersion coefficient due to gap states absorption, $\tau = t - z/\upsilon_g$ notes the retarded time, υ_g is the group-velocity without absorption, $\xi = z$ notes a coordinate in the moving frame, T_{10} is the lifetime of gap states, T_{20} and T_{21} are the lifetimes of the conduction band relative to the valence band and gap states, t is the time, z is the distance. According to the conditions and approaches of Ref.11, these equations can be simplified into,

$$\frac{\partial}{\partial \tau} N_1 = \frac{1}{2}\sigma_{01}^{(2)} N I^2 - \frac{1}{T_{10}} N_1, \qquad (5)$$

$$\frac{\partial}{\partial \xi} I = -\sigma_{12}^{(1)}(N_1 - N_2)I - \delta_{01}^{(2)}(N_0 - N_1)I\frac{\partial}{\partial \tau} I - \delta_{12}^{(1)}(N_1 - N_2)\frac{\partial}{\partial \tau} I. \qquad (6)$$

For the ZnSe plate used in our experiment, the second term in the right hand of Eq.(5) and the third term in the right hand of Eq.(6) can be neglected because the lifetime of gap states is much longer than the width of incident pulse and the linear dispersion corresponding to the wide band absorption of gap states is small. Supposed

$\sigma_{01}^{(2)}\sigma_{12}^{(1)}N = 4\times10^{-12}$ m/s/W^2 and $\delta_{01}^{(2)} = -3.8\times10^{-21}$ sm/W, the reshaping of the laser pulse through the ZnSe plate is shown in Fig.4. Curve A is the incident pulse with the Gaussian profile, curve B is the transmitted pulse after two-step absorption without nonlinear dispersion, and curve C is the transmitted pulse after two-step absorption with nonlinear dispersion. For the sake of contrast, curve D shows the transmitted pulse after pure three-photon absorption.

Briefly, with the help of our developed single-shot Kerr gate technique, the time advancement and temporal narrowing of the propagating pulse have been observed at the incident pulse peak intensity of 3.65GW/cm^2 in a ZnSe plate. The negative nonlinear dispersion was obtained based on the intensity-dependent peak-shift of the propagating pulse. Time-dependent transmission of a 1064-nm laser pulse through ZnSe shows that the nonlinear absorption in ZnSe at 1064 nm is not a simple three-photon absorption process. Based on the model of two-step absorption with negative nonlinear dispersion, the experimental results have been fitted. These data weren't obtained by conventional nonlinear measurement technique, such as Z-scanning. It will be very useful in studying the properties and seeking the application of ZnSe.

This research is supported in part by AF Wright Laboratory, NYSTAR and ARO.

References:

1. G.R.Olbright, N. Peyghambarian, H. M. Gibbs, H.A. Macleod, and F. Van Milligen, Appl. Phys. Lett. **45** (1984) 1031.
2. I. Janossy, M.R. Taghizadeh, J. G. H. Mathew, and S.D. Smith, IEEE J. Quantum Electron. **QE-21** (1985) 1447.
3. E. W. Van Stryland, H. Vanherzeele, M. A. Woodall, M. J. Soileau, A. L. Smirl, S. Guha, and T. F. Boggess, Opt. Eng. **24** (1985) 613.
4. M. Sheik-Bahae, D. C. Hutchings, D. J. Hagan, and E. W. Van Stryland, IEEE J. Quantum Electron., **QE27** (1991) 1296.
5. M. Sheik-Bahae, A. A. Said, T. Wei, D. J. Hagan, and E. W. Van Stryland, IEEE J. Quantum Electron., **QE26** (1990) 760.
6. K. W. Berryman, and C. W. Rella, Phys. Rev. **B 55** (1997) 7148.
7. R. R. Alfano, Q. Z. Wang, T. Jimbo, P.P. Ho, R.N. Bhargava and B. J. Fitzpatrick, Phys. Rev. **A35** (1987) 459.
8. E. B. Treacy, Phys.Lett. **28A** (1968) 34.
9. P. P. Ho, and R. R. Alfano, Physics. Rev. **A20** (1979) 2170.
10. Yingxin Bai, Fanan Zeng, P. P. Ho and R. R. Alfano, a report to be submitted on "Intensity-dependent group velocity, self-steepening and asymmetry of the spectral broadening of laser pulses in a nonlinear dispersion medium", gives the intensity-dependent group-velocity: $\upsilon_g(\omega, I) = \frac{c}{n + \omega\frac{\partial n}{\partial \omega} + 6n_2 I + \frac{3\omega}{n}\left(\frac{\partial (n_2 n)}{\partial \omega}\right)I}$, and the time-delay

of the pulse peak: $\Delta\tau = \frac{L}{c}\left(6n_2 + \frac{3\omega}{n}\left(\frac{\partial(n_2 n)}{\partial\omega}\right)\right)\Delta I$, where $\Delta\tau < 0$ indicates the steepening of the leading-edge of the pulse, while $\Delta\tau > 0$ indicates the steepening of the trailing-edge of the pulse. In addition, $\Delta\tau/n_2 < 0$ gives a larger Stokes spectral broadening than anti-Stokes, and $\Delta\tau/n_2 > 0$ gives a larger anti-Stokes spectral broadening than Stokes.

11. J. Herrmann, J. Wienecke, B. Wilhelmi, Optical and Quantum Electronics **7** (1975) 337.

Figure Captions:

Figure 1: Single shot optical Kerr gate experimental setup. A mode locked YAG laser generates the 1064nm laser pulses of ~40 ps in FWHM, the laser pulses pass through the second harmonic crystal (KDP) generating 532nm laser pulses of ~30ps in FWHM. These pulses are split into a pumping beam (1064nm) and a probing beam (532nm) by a beam splitter (BS). The probing beam reflected by mirrors M_1 and M_2 reaches a 6-cm long 90° blazed grating with 1800lines/mm. For improving the spatial uniformity of the probing beam only a 3-mm central portion of the 9-mm diameter probing beam is diffracted into a ~200ps oblique wave front. The segmented pulse passes through lens L_3, the Kerr gate and lens L_4 and reaches a cooled charge coupled device (CCD) camera with 1024×1024 pixels and a 16 bit dynamic range. This pulse is used to probe the 1064-nm pulse profile. The Kerr gate is composed of a pair of crossed Polaroid (HN22) polarizers P_2 and P_3 and a 1-mm thick CS_2 cell located at the focal point of lens L_3 as the Kerr medium. The focal lengths of lens L_3 and L_4 are 20 cm. The pumping beam passes into a delay line composed of mirrors M_3 and M_4 and a movable prism and passes through a series of neutral density filters (F) and a 30-cm focal length lens (L_1) into the ZnSe sample. The 1064-nm pumping beam passes through another 30-cm focal-length lens L_2 and meets the 532-nm probing beam in the CS_2 Kerr medium. The 532-nm beam diameter is 1mm and is located at the center of the 1064-nm pumping beam of 3-mm in diameter. The 1064-nm laser beam is directed into an energy/power meter (D).

Figure 2: Single-shot OKG temporal profiles of a 40-ps 1064-nm pulse passing through a

3-mm ZnSe plate when the peak intensity of the incident pulse reaches 0.365 GW/cm^2, 1.46 GW/cm^2 and 3.65 GW/cm^2.

[Upper left insert] Single-shot OKG temporal profiles of a 40-ps 1064-nm pulse passing through 3-mm glass at intensities 0.365 GW/cm^2, 1.46 GW/cm^2 and 3.65 GW/cm^2.

[Upper right insert] The transmissivity of a 3-mm ZnSe plate without coating as a function of wavelength.

Figure 3: The transmitted hysteresis of a single 1064-nm laser pulse through a 3-mm thick ZnSe plate at the peak intensity of an incident pulse of 3.65 GW/cm^2.

Figure 4: Theoretical calculations: Curve A is the incident pulse with the Gaussian profile, curve B is the transmitted pulse after two-step absorption without nonlinear dispersion, curve C is the transmitted pulse after two-step absorption with nonlinear dispersion; and curve D is the transmitted pulse after pure three-photon absorption.

[Insert] The energy level diagram of two-step absorption, two-photon absorption between valence band and gap states and time (τ_0) delayed single-photon absorption from gap states to conduction band.